

Performance enhancement of AlGa_N deep-ultraviolet light-emitting diodes with varied superlattice barrier electron blocking layer

Songqing Liu¹ · Chunya Ye¹ · Xuefen Cai¹ · Shuping Li¹ · Wei Lin¹ · Junyong Kang¹

Received: 9 February 2016 / Accepted: 15 April 2016 / Published online: 26 April 2016
© Springer-Verlag Berlin Heidelberg 2016

Abstract The AlGa_N-based deep-UV LEDs with specific design of varied superlattice barrier electron blocking layer (EBL) has been investigated numerically by APSYS software. The proposed structure exhibits significant improvement in the light output power, internal quantum efficiency, current–voltage curve and electroluminescence intensity. After analyzing the profiles of energy band diagrams, carriers concentration and radiative recombination rate, we find the main advantages of proposed structure are ascribed to higher barrier suppressing electron leakage and reduced barrier for hole injection. Thus, compared with reference sample, the proposed EBL design may be a good method for improving the whole performance of UV LEDs.

1 Introduction

In recent decades, direct-gap III–V nitride semiconductor has been widely used in optoelectronic devices. As high-brightness blue LEDs continue to mature, much attention riveted on high-aluminum component UV LEDs because of their wide range of potential applications like air and water purification [1], germicidal and biomedical instrumentation systems [2], full color display, optical data storage [3] and white emission lighting [4]. However, the EQEs of reported Al_xGa_{1-x}N deep-UV LEDs with emission wavelengths from 227 to 280 nm are typically less than 10 % [5, 6].

Multiple causes are responsible for the low efficiency. The high dislocation density in AlGa_N materials grown on sapphire substrate will lead to non-radiative recombination in the active region; large spontaneous and piezoelectric polarization charges generated in the heterointerfaces can largely influence the mobile carriers injection and band structure; high ionization energy of Mg acceptor and strong electron leakage phenomenon is also regarded as an important factor decreasing the internal quantum efficiency (IQE). To overcome the block, some methods have been developed, for instance, nano-patterned substrate has been adopted to reduce dislocation densities in AlN and epilayers above [7]. As for the latter two problems, researchers often try to modulate energy band structure to improve the performance of LEDs, for instance, passivating graphene oxide on top of the fully fabricated LED [8], graded-composition multiple quantum barriers [9], staggered QWs [10] and polarization-induced hole doping [11]. Through these processes, the radiative recombination rate can be enhanced owing to increased electron–hole wave function overlap and carriers injection rate.

Actually, the region between multiple quantum wells and p-type layer plays a very important role in the whole performance of LEDs as carriers tend to accumulate in this region and holes inject through the barrier height from p-type layer. People has paid much attention to optimize the structure here; Yang et al. found that Al content graded AlGa_N electron blocking layer inserted between multiple quantum wells and p-type layer can improve the overall device performance [12]. Jun et al. pointed out that inserting a p-AlGa_N layer between the electron blocking layer and the last barriers of the MQWs can be a good solution [13]. In our previous work, we also proposed structures achieving remarkable improvement in UV LEDs like using p-type and thickened last quantum barrier [14].

✉ Shuping Li
lsp@xmu.edu.cn

¹ Fujian Provincial Key Laboratory of Semiconductors and Applications, Collaborative Innovation Center for Optoelectronic Semiconductors and Efficient Devices, Department of Physics, Xiamen University, Xiamen 361005, People's Republic of China

In this study, we seek to find a preferable designing approach of superlattice EBL with varied barrier component, while the overall performance improves tremendously compared to the samples with traditional superlattice EBL design reported by researchers earlier [15, 16].

The properties of referenced structure and proposed structure are investigated numerically in detail with the Advance Physical Model of Semiconductor Devices simulation program developed by Crosslight Software, Inc. To explain the mechanism, we have simulated optical and electrical properties, band diagram and carriers concentration by solving the Poisson's equation, the Schrödinger equation, the carrier transport equations and the current continuity equation self-consistently [17, 18].

2 Model and parameters

As shown in Fig. 1, the reference sample with a superlattice EBL is marked as Sample A, which is designed to be grown on c-sapphire substrate, followed by a 1- μm -thick AlN buffer and 1.4- μm -thick n-doped $\text{Al}_{0.5}\text{Ga}_{0.5}\text{N}$ layer. The active region consists of six 10-nm-thick undoped $\text{Al}_{0.45}\text{Ga}_{0.55}\text{N}$ barriers and five 3-nm-thick undoped $\text{Al}_{0.35}\text{Ga}_{0.65}\text{N}$ wells. Then a superlattice EBL containing six 2-nm-thick p-doped $\text{Al}_{0.85}\text{Ga}_{0.15}\text{N}$ barriers and five 2-nm-thick undoped $\text{Al}_{0.6}\text{Ga}_{0.4}\text{N}$ wells is employed on the top of active region in order to decrease the electron leakage. A 10-nm-thick p-type $\text{Al}_{0.5}\text{Ga}_{0.5}\text{N}$ layer and a 1.4- μm -thick p-type GaN contact layer are eventually grown. Although the use of high-Al component in the barriers of EBL will cause increased resistance, the advantages such as quantum effect [19] and carrier tunneling [20] brought by superlattice EBL may reduce the negative effect, while

in structure B, the Al component of superlattice EBL barrier is linearly varied from 90 to 65 % (as depicted in Fig. 1). Except for that, the other regions are kept identical between structure A and structure B. The process of selecting the optimized proposed structure will be discussed in detail below.

In the simulation, the equilibrium temperature was assumed to be 350 K, and the band-offset ratio was assumed to be 0.5 for AlGaN materials [21]. The Auger recombination coefficient was set to $1 \times 10^{30}\text{cm}^6$ to fit the experiment [20]. The Shockley–Read–Hall (SRH) recombination time was set to 1.5 ns [22]. The polarization effect of $\text{Al}_x\text{Ga}_{1-x}\text{N}$ alloy with wurtzite structure was considered using the same model as Fiorentini et al., with 50 % interface charge density in calculated value. The other detailed material parameters can be found in [23].

3 Results and discussions

Firstly, we try to find out the optimized multiple Al component of superlattice barrier in EBL. Table 1 summarizes the values of the Al component of superlattice well and barrier of EBL, along with efficiency droop and maximum power. As we know, higher Al component will lower the conductivity but increase effective barrier height of EBL, both of which will influence the emitting efficiency of LEDs. Column 1 matches well with Sample A; we, respectively, increase and decrease the barrier component to 0.9 and 0.8 that can be seen clearly in Column 2 and 3, but the performance becomes worse than Column 1. It can be found that conductivity and barrier height may be in a competitive mechanism that influences the performance of LEDs; thus, we should find out the best match situation. After that, we introduce new designs of multi-superlattice

Fig. 1 Schematic diagrams of original UV LED with a superlattice EBL (Sample A) and proposed UV LED with varied superlattice barrier EBL (Sample B)

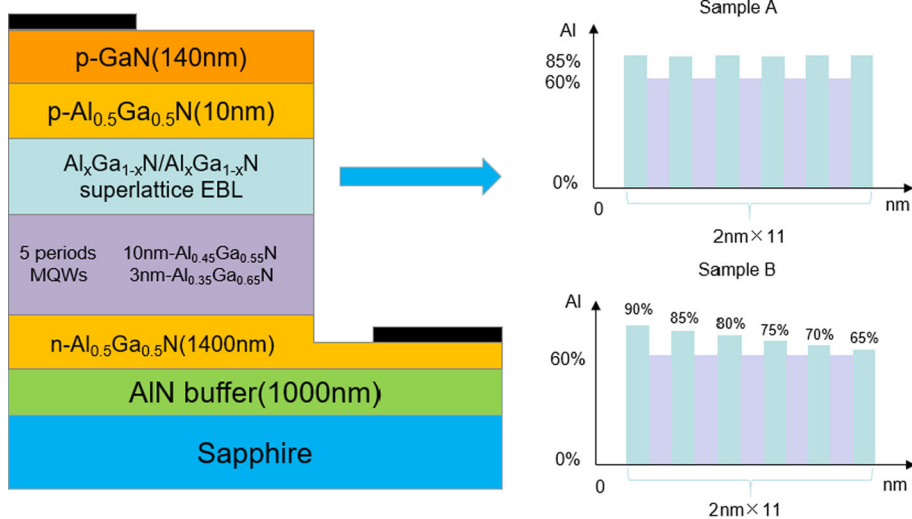


Table 1 Values of Al component of superlattice well and barrier of EBL, along with efficiency droop and maximum power

Column	Well (×5)	Barrier (along the growth direction)						Efficiency drop (%)	Maximum power (mW)
1	0.6	0.85	0.85	0.85	0.85	0.85	0.85	80.8	159
2	0.6	0.90	0.90	0.90	0.90	0.90	0.90	89.2	79.5
3	0.6	0.80	0.80	0.80	0.80	0.80	0.80	82.1	138
4	0.6	0.90	0.85	0.80	0.75	0.70	0.65	28.8	637.5
5	0.6	0.65	0.70	0.75	0.80	0.85	0.90	98.2	7.7
6	0.6	0.80	0.85	0.90	0.85	0.80	0.75	64.6	292.5
7	0.6	0.95	0.85	0.80	0.75	0.70	0.65	40.8	510
8	0.6	0.92	0.87	0.82	0.77	0.72	0.67	37.5	540
9	0.6	0.88	0.83	0.78	0.73	0.68	0.63	49.3	435

barrier EBL, and the Al component varied from 0.90 to 0.65 in Column 4, 0.65 to 0.90 in Column 5, stepwise from 0.80 to 0.9 and decreases to 0.75 in Column 6. Column 4 is the corresponding structure of Sample B, which shows the best performance (efficiency droop = 28.8 %, maximum power = 637.5 mW) among all. We believe that higher Al component in the first barrier of EBL will enhance the electron blocking effect because of higher effective barrier height. In order to confirm whether the main factor is it or not, we increase the component of first barrier to 95 % in Column 7 (the rest remains consistent with Column 4), but the results were not in the expected. Lastly, we increase and decrease the component of each barrier by 2 % as shown in Column 8 and 9, and the output results both dropped. So far, we have found an optimized EBL structure owning linearly varied barrier component as shown in Column 4, while the conductivity and effective barrier height of EBL reached a balance improving the performance of UV LEDs.

In order to make a comparison of Sample A and Sample B, we have carried out APSYS simulation on light output power, internal quantum efficiency (IQE), current–voltage curve (IV), electroluminescence intensity (EL), band diagrams, carrier concentration and radiative recombination rate for discussion.

Figures 2 and 3 show the light output power and IQE as functions of the injection current for the two samples. As shown in Fig. 2, the simulated output power of Sample A and Sample B both increases with injection current, but Sample B increases faster than Sample A, especially under higher injection current. The specific values are, respectively, 159 and 637.5 mW at 300 mA. The higher output power may ascribe to increased carriers confinement in the active region and increased hole injection from p-type layer, which will be clarified in next pages. In Fig. 3, we can find that along with the increase in injection current, Sample B exhibits lower efficiency droop than Sample A. In the whole injection current range, the efficiency droop in Sample B is 28.8 %, while Sample A is 80.8 %, when the

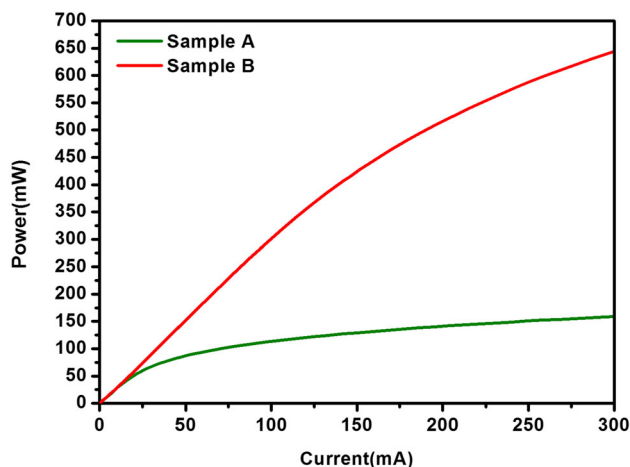


Fig. 2 Light output power as a function of injection current for Sample A and Sample B

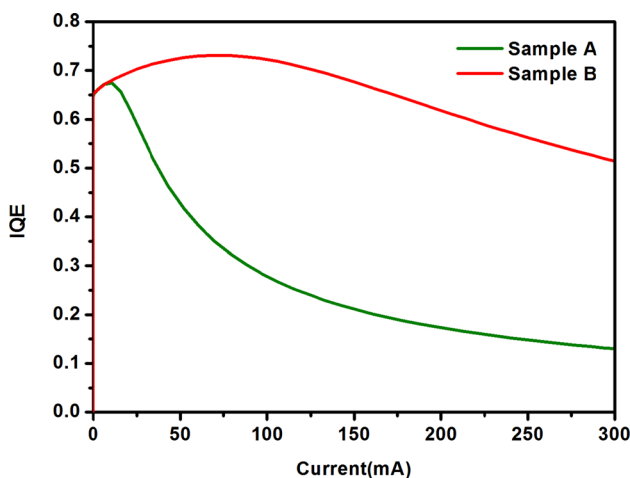


Fig. 3 Internal quantum efficiency as a function of injection current for Sample A and Sample B

efficiency is defined as $(IQE_{max} - IQE_{300\text{ mA}})/IQE_{max}$. Figure 3 corresponds well with Fig. 2, indicating that such a treatment in superlattice electron blocking layer is

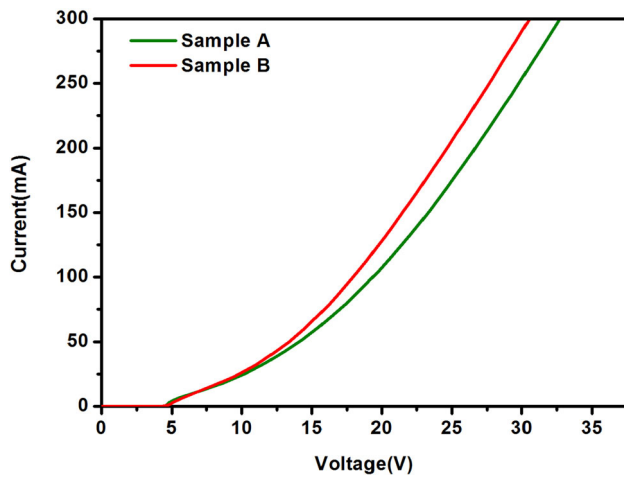


Fig. 4 Forward current–voltage curve for Sample A and Sample B

important to obtain superior performance of nitride-based UV LEDs.

Figure 4 shows the I–V curve of Sample A and Sample B. The turn-on voltage of Sample A and Sample B is nearly the same at about 4.7 V. But the forward voltage of the two samples at 150 mA is 23.2 and 21.5 V, demonstrating that Sample A owning higher resistance, which is likely attributed to higher activation energy of Mg and higher average Al component. The electroluminescence spectra are illustrated in Fig. 5. It can be seen that both samples show one emission peak around 298 nm, indicating that there was no radiative recombination occurred in other region. We can calculate that the electroluminescence density of Sample B is 175.7 % higher than Sample A, which suggests that Sample B owns better optical performance using varied superlattice barrier electron blocking layer.

After presenting the simulation results of light output power, internal quantum efficiency (IQE), current–voltage curve (IV) and electroluminescence density (EL) of Sample A and Sample B, we should try to shed light on the mechanism as clearly as possible. Figure 6 plots the energy band diagrams and quasi-Fermi levels for Sample A and Sample B. As we know, energy band bending makes electron wave function and hole wave function more dispersed. In addition, due to large difference in polarization between the last $\text{Al}_{0.45}\text{Ga}_{0.55}\text{N}$ barrier and the EBL layer, high density of positive polarization charges exist at their interface, which attracts electrons from the n-type side and repel holes from the p-type [12]. So it is easy to understand the difficulty of carriers confinement in active region and hole injection from p-type layer. As marked in Fig. 6a, we can find out that a potential barrier height of 568 meV is present between last quantum barrier and p-type layer in Sample A; the corresponding value in Sample B is 699 meV. It means that Sample B can suppress electron

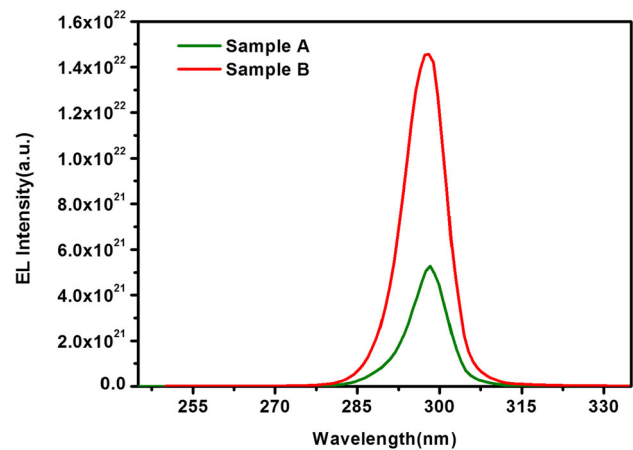


Fig. 5 Electroluminescence spectra for Sample A and Sample B

overflow more effectively, thus increasing the radiative recombination rate in the active region. At the same time, the effective potential height for holes in valence band reduces from 506 to 487 meV as marked in Fig. 6b, which can be beneficial for hole injection from p-type layer. Consequently, when the Al component of superlattice EBL barrier is linearly varied from 90 to 65 %, it can not only increase the effective barrier height of the conduction band but also decrease obstacle barrier height for hole injection in the valence band. Moreover, the conductivity of EBL is improved undoubtedly due to lower Al component on the whole, which is beneficial for the output performance.

The explanation can be confirmed by the profiles of carriers concentration across active region and p-type region in Fig. 7. As shown in Fig. 7a, the electron concentration in active region is nearly the same, but compared to Sample A, electron concentration of Sample B in p- $\text{Al}_{0.5}\text{Ga}_{0.5}\text{N}$ layer is much lower, indicating that the specially designed EBL is helpful to reduce electron leakage into p-type layer. In Fig. 7b, the hole concentration of Sample B is higher than Sample A across the active region, which may be ascribed to lower barrier for holes injection in the valence band. Apparently, the design of varied superlattice barrier electron blocking layer increased both electrons and holes concentrations in the active region of Sample B.

At last, Fig. 8 plots the corresponding radiative recombination rates of Sample A and Sample B. Due to the increment of electrons and holes concentrations in the active region, the radiative recombination rates across five quantum wells are significantly enhanced when the superlattice EBL is replaced by varied barrier superlattice EBL.

According to the analysis above, energy band diagrams, carriers concentration and radiative recombination rates have been presented. It is believed that due to optimization of EBL structure, more electrons and holes survived and

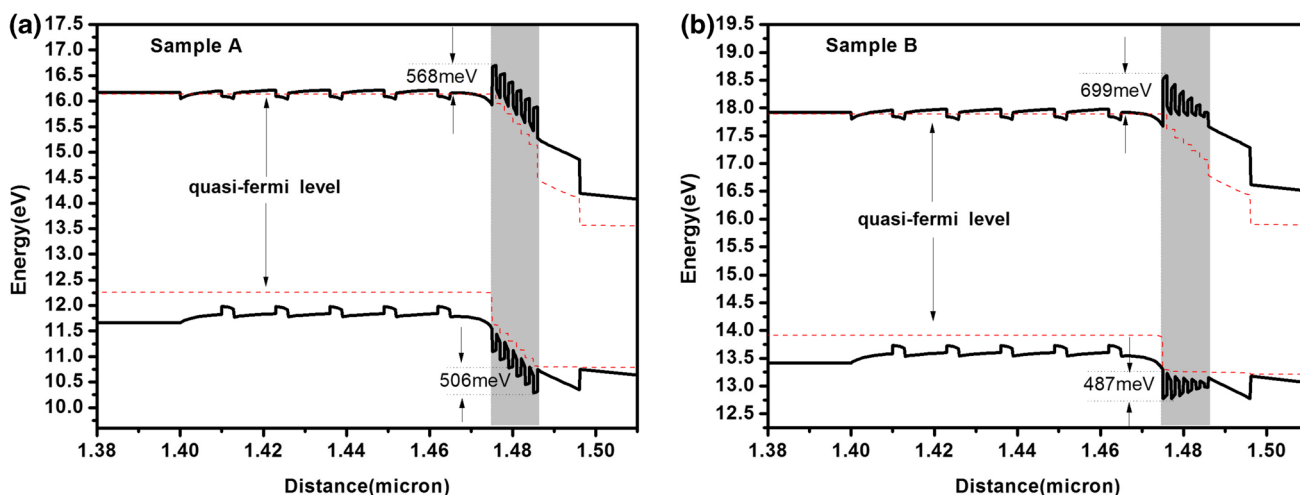


Fig. 6 Energy band diagrams of a Sample A and b Sample B

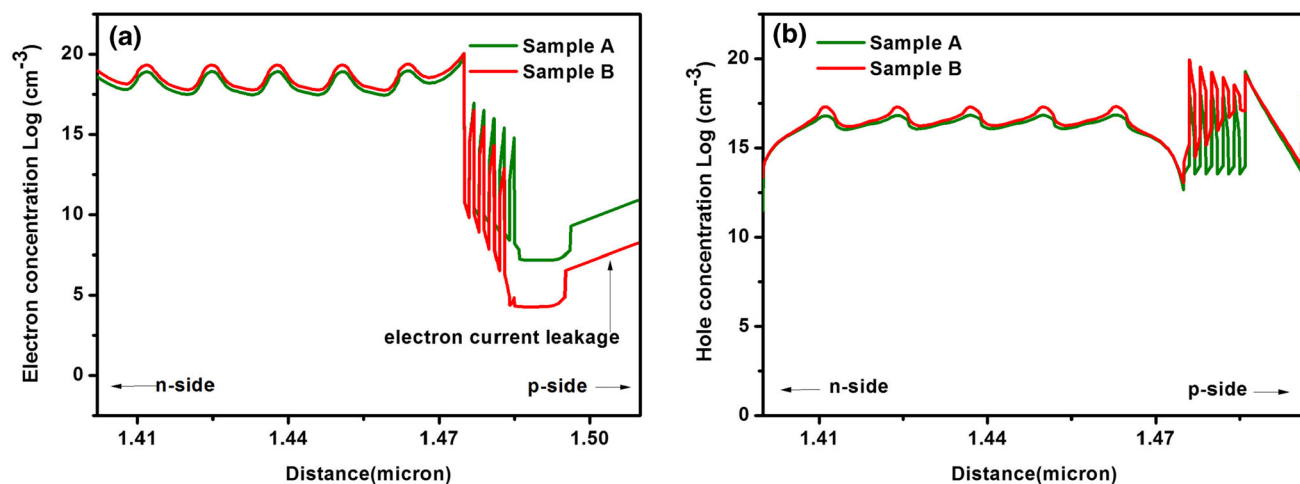


Fig. 7 Distribution of a electron concentration and b hole concentration of Sample A and Sample B

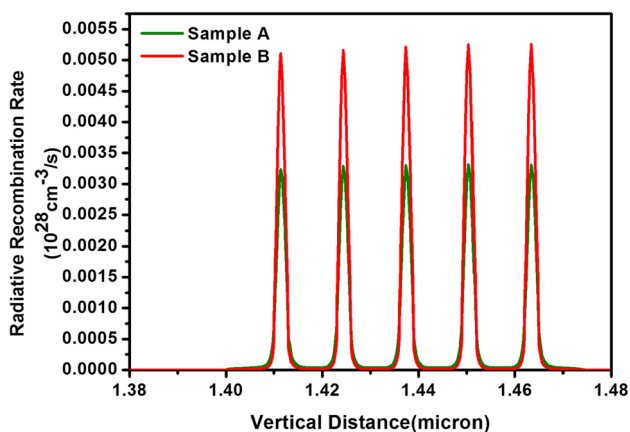


Fig. 8 Radiative recombination rates of a Sample A and b Sample B

accumulated in the active region, which contributes to

higher radiative recombination rate; thus, the whole performance improved in Sample B.

4 Conclusions

In this paper, design and characterization of deep-UV LEDs with varied superlattice barrier electron blocking layer was investigated. Light output power, internal quantum efficiency, current–voltage curve and electroluminescence intensity, band diagrams, carrier concentration and radiative recombination rate were analyzed. Simulation results show that varied superlattice barrier electron blocking layer has a greater advantage than common superlattice electron blocking layer (the output power improved about 301 % at 300 mA, IQE droop decreased from 80.8 to 28.8 %, and EL intensity improved about

175.7 %), which we attribute to three main factors: (1) higher effective barrier in the conduction band suppressing the spillover of electrons out of active region; (2) holes injection improvement due to lower potential height in the in valence band; and (3) lower resistivity of the structure due to lower Al component on the whole. To conclude, the design presented here could be a useful reference to produce high-Al component UV LEDs owning better performance.

Acknowledgments This work was supported by the ‘973’ Program (2012CB619301), the ‘863’ Program (2014AA032608), the National Natural Science Foundation of China (11204254) and the Fundamental Research Funds for the Central Universities (2012121014).

References

1. Y.-S. Tang, S.-F. Hu, C.C. Lin, N.C. Bagkar, R.-S. Liu, *Appl. Phys. Lett.* **90**, 151108 (2007)
2. S.J. Kim, T.G. Kim, *Phys Status Solidi (a)* **211**, 656 (2014)
3. C. Pernot, M. Kim, S. Fukahori, T. Inazu, T. Fujita, Y. Nagasawa, A. Hirano, M. Ippommatsu, M. Iwaya, S. Kamiyama, I. Akasaki, H. Amano, *Appl. Phys. Express* **3**, 061004 (2010)
4. D. D. Doxsee and C. Jacob, (Google Patents, 2004)
5. M. Shatalov, W. Sun, A. Lunev, X. Hu, A. Dobrinsky, Y. Bilenko, J. Yang, M. Shur, R. Gaska, C. Moe, G. Garrett, M. Wraback, *Appl. Phys. Express* **5**, 082101 (2012)
6. H. Hirayama, S. Fujikawa, N. Noguchi, J. Norimatsu, T. Takano, K. Tsubaki, N. Kamata, *Phys. Status solidi (a)* **206**, 1176 (2009)
7. P. Dong, J. Yan, J. Wang, Y. Zhang, C. Geng, T. Wei, P. Cong, Y. Zhang, J. Zeng, Y. Tian, L. Sun, Q. Yan, J. Li, S. Fan, Z. Qin, *Appl. Phys. Lett.* **102**, 241113 (2013)
8. H. Jeong, S.Y. Jeong, D.J. Park, H.J. Jeong, S. Jeong, J.T. Han, H.J. Jeong, S. Yang, H.Y. Kim, K.J. Baeg, S.J. Park, Y.H. Ahn, E.K. Suh, G.W. Lee, Y.H. Lee, M.S. Jeong, *Sci. Rep.* **5**, 7778 (2015)
9. C.H. Wang, S.P. Chang, P.H. Ku, J.C. Li, Y.P. Lan, C.C. Lin, H.C. Yang, H.C. Kuo, T.C. Lu, S.C. Wang, C.Y. Chang, *Appl. Phys. Lett.* **99**, 171106 (2011)
10. R.A. Arif, Y.-K. Ee, N. Tansu, *Appl. Phys. Lett.* **91**, 091110 (2007)
11. S.D. Carnevale, T.F. Kent, P.J. Phillips, M.J. Mills, S. Rajan, R.C. Myers, *Nano Lett.* **12**, 915 (2012)
12. L. Yang, C. Shengchang, T. Wu, W. Zhihao, F. Yanyan, D. Jiangnan, C. Changqing, *IEEE Photonics J.* **5**, 8200309 (2013)
13. Z. Jun, T. Wu, W. Feng, Y. Weiyi, X. Hui, D. Jiangnan, F. Yanyan, W. Zhihao, C. Changqing, *IEEE Photonics J.* **5**, 1600310 (2013)
14. X. Bao, P. Sun, S. Liu, C. Ye, S. Li, J. Kang, *IEEE Photonics J.* **7**, 1 (2015)
15. C. Liu, T. Lu, L. Wu, H. Wang, Y. Yin, G. Xiao, Y. Zhou, S. Li, *IEEE Photonics Technol. Lett.* **24**, 1239 (2012)
16. Y.Y. Zhang, Y.A. Yin, *Appl. Phys. Lett.* **99**, 221103 (2011)
17. S.-H. Yen, M.-C. Tsai, M.-L. Tsai, Y.-J. Shen, T.-C. Hsu, Y.-K. Kuo, *IEEE Photonics Technol. Lett.* **21**, 975 (2009)
18. Y.Y.K. Kuo, M.C. Tsai, S.H. Yen, T.C. Hsu, Y.J. Shen, *IEEE J. Quantum Electron.* **46**, 1214 (2010)
19. S.N. Lee, S.Y. Cho, H.Y. Ryu, J.K. Son, H.S. Paek, T. Sakong, T. Jang, K.K. Choi, K.H. Ha, M.H. Yang, *Appl. Phys. Lett.* **88**, 111101 (2006)
20. C.S. Xia, Z.S. Li, Z. Li, Y. Sheng, *Appl. Phys. Lett.* **102**, 013507 (2013)
21. W. Tian, Z. Feng, B. Liu, H. Xiong, J. Zhang, J. Dai, S. Cai, C. Chen, *Opt. Quant. Electron.* **45**, 381 (2013)
22. K. Baik, Y. Irokawa, F. Ren, S. Pearton, S. Park, Y. Park, *Solid-State Electron.* **47**, 1533 (2003)
23. L. Zhang, X. Wei, N. Liu, H. Lu, J. Zeng, J. Wang, Y. Zeng, J. Li, *Appl. Phys. Lett.* **98**, 241111 (2011)